

Alkylation of Guanine in DNA by S23906-1, a Novel Potent Antitumor Compound Derived from the Plant Alkaloid Acronycine[†]

Marie-Hélène David-Cordonnier,[‡] William Laine,[‡] Amélie Lansiaux,[‡] Mostafa Kouach,[§] Gilbert Briand,[§] Alain Pierré,^{||} John A. Hickman,^{||} and Christian Bailly^{*,‡}

INSERM U-524 et Laboratoire de Pharmacologie Antitumorale du Centre Oscar Lambret, IRCL, Lille 59045, Laboratoire de Spectrométrie de Masse, Université de Lille II, Lille 59045, and Division de Cancérologie, Institut de Recherches SERVIER, Suresnes 92150, France

Received March 21, 2002; Revised Manuscript Received May 24, 2002

ABSTRACT: The discovery of a new DNA-targeted antitumor agent is a challenging enterprise, and the elucidation of its mechanism of action is an essential first step in investigating the structural and biological consequences of DNA modification and to guide the rational design of analogues. Here, we have dissected the mode of action of the newly discovered antitumor agent S23906-1. Gel retardation experiments reveal that the diacetate compound S23906-1 and its monoacetate analogue S28687 form highly stable covalent adducts with DNA. The covalent adducts formed between S23906-1 and a 7-bp hairpin oligonucleotide duplex were identified by spectrometry. In contrast, the inactive compound S23907, lacking the two acetate groups of S23906-1, fails to yield covalent DNA adducts, indicating that the C1–C2 functionality is the DNA reactive moiety. DNase I footprinting and DNA alkylation experiments indicate that S23906-1 reacts primarily with guanine residues. A 30-mer oligonucleotide containing only G·C bp forms highly stable complexes with S23906-1 and S28687, whereas the equivalent A·T oligonucleotide is not a good substrate for these two drugs. The use of an oligonucleotide duplex containing inosines instead of guanines identifies the guanine 2-amino group exposed in the minor groove of DNA as the potential reactive site. The reactivity of S23906-1 toward the guanine-N2 group was independently confirmed by fluorescence spectroscopy. Covalent DNA adducts were also identified in the genomic DNA of B16 melanoma cells exposed to S23906-1, and the specific accumulation of the drug in the nucleus of the cells was visualized by confocal microscopy. The elucidation of the mechanism of action of this highly potent anticancer agent opens a new field for future drug design.

Cancer chemotherapy relies to a great extent on the use of drugs which interact with DNA or interfere with DNA metabolism (1, 2). Drugs derived from natural products still represent an attractive source for antitumor agents, due to the tremendous chemical diversity and, consequently, the variety of mechanisms of action potentially involved. The alkaloid acronycine was originally isolated from the bark of the Australian scrub ash *Acronychia baueri* (3, 4). Acronycine itself has shown moderate cytotoxicity against certain tumor cells in vitro and exhibited only weak antitumor activity in vivo (5). Structure–activity relationship studies have led recently to the total synthesis of acronycine derivatives with markedly improved pharmacological properties (6, 7) but, however, without any knowledge of their molecular mechanism of action. Among these potent compounds, S23906-1, a benzoacronycine derivative bearing two

acetate groups at positions 1 and 2 (Figure 1) was selected for further evaluation. This derivative displayed an unusual pharmacological profile in vivo in that it was markedly active in orthotopic models of human solid tumors, even by the oral route, but only moderately active against murine transplantable tumors (8). It induces specific cell cycle perturbations and promotes apoptosis in different cancer cell lines (9). Interestingly, an early increase of cyclin E accompanied by inhibition of DNA synthesis appeared to be closely linked to the cytotoxic properties of S23906-1 (9). S23906-1 thus stands as a promising candidate for clinical trials, but its molecular mechanism of action remains to be solved, at least for a rational positioning in a clinical setting.

Acronycine inhibits DNA and RNA synthesis, possibly as a result of its potential capacity to intercalate into DNA (10–13). By analogy, we reasoned that S23906-1 may also interact with DNA. Here, we present the results of our studies revealing that, unexpectedly, S23906-1 and its monoacetate derivative S28687 alkylate DNA, at the guanine-N2. The diol derivative S23907 (Figure 1), which is inactive in vitro and in vivo (7), shows no DNA binding capacity. Our demonstration that S23906-1 forms DNA covalent adducts at guanine-N2 in the minor groove elucidates the potential mechanism of action through which this promising com-

[†] This work was done under the support of a Servier research grant to C.B. and a fellowship to M.-H.D.-C. from the Association pour la Recherche sur le Cancer.

* Corresponding author address: INSERM U-524, Institut de Recherches sur le Cancer, 1 Place de Verdun, Lille 59045, France. Phone: +33 320 16 92 18. Fax: +33 320 16 92 29. E-mail: bailly@lille.inserm.fr.

[‡] INSERM U-524.

[§] Université de Lille II.

^{||} Institut de Recherches SERVIER.

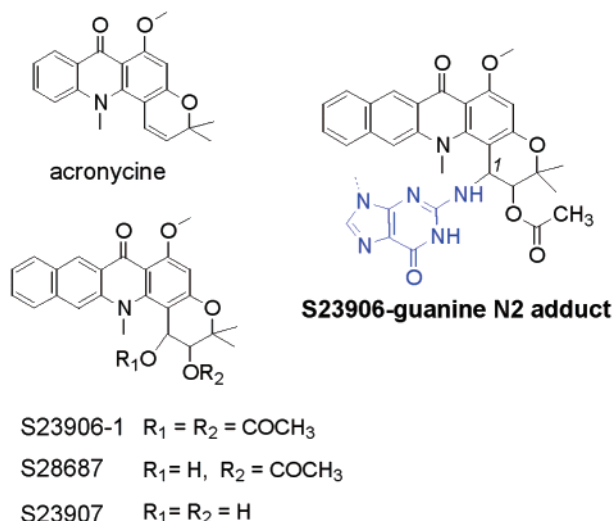


FIGURE 1: Structure of acronycine, the three synthetic derivatives used in this study, and the proposed S23906-1-guanine-N2 adduct.

pound exerts its unusual profile of antitumor activity. Its ability to produce covalent adducts with both purified DNA and genomic DNA in cells represent a significant elucidation of the mechanism of action of this family of anticancer agents, opening thus a new field for future drug design.

MATERIALS AND METHODS

Chemicals and Biochemicals. The synthesis of the benzo-acronycine derivatives S23906-1, S28687, and the diol S23907 has been reported recently (7). To prepare the AT, IC, and GC targets, a synthetic 30-mer oligonucleotide [d(TATATATAAAATATATATTTAAATATATA), d(CGCCGCGGGGCGCGCGCCCGGGCGCGCG), and d(5'-CICICICIIICICICICCCIIICICICI)] and its complement were mixed at a 1:1 ratio, heated to 70 °C, and slowly cooled to form duplex which was then labeled at the 3' end using α -[³²P]-dATP or α -[³²P]-dCTP (3000 Ci/mmol) and AMV reverse transcriptase. Unincorporated radionucleotides were removed by using a G25 sephadex spin column.

DNA Restriction Fragments. The pBS and pKS plasmids were digested with *Pvu*II and *Eco*RI, and the resulting 117-bp¹ and 174-bp fragments were labeled at the *Eco*RI site with α -[³²P]-dATP and AMV reverse transcriptase. Electrophoresis on a nondenaturing 6% (w/v) polyacrylamide gel served to remove excess radioactive nucleotide, with the desired 3'-end-labeled product being cut out of the gel and eluted overnight in 500 mM ammonium acetate and 10 mM magnesium acetate.

Gel Shift Studies. A typical cross-linking reaction consisted in incubating 8 μ L of radiolabeled DNA, 2 μ L of buffer (10 mM sodium cacodylate (pH 7.0); Tris buffer must be avoided due to the presence of reactive amine functions), and 10 μ L of the drug at the desired concentration for 1 or 15 h in the dark at room temperature prior to adding 5 μ L of a 50% glycerol solution containing tracking dyes. DNA samples were resolved by electrophoresis under nondenaturing conditions in 6% or 10% acrylamide gels for about 5 h at 300 V at room temperature in TBE buffer (89 mM Tris base, 89 mM boric acid, 2.5 mM Na₂EDTA (pH 8.3)). Gels were

transferred to Whatman 3MM paper, dried under vacuum at 80 °C, and then analyzed on the phosphorimager (Molecular Dynamics 445SI, Molecular Dynamics, Cleveland, OH).

DNase I Footprinting. Samples (3 μ L) of the labeled 174-bp DNA fragment were incubated with 5 μ L of the buffered solution containing the ligand at an appropriate concentration. After 15 h incubation at room temperature in the dark, the digestion was initiated by the addition of 2 μ L of a DNase I solution (final concentration of 0.01 unit/mL). After 3 min, the reaction was stopped by the addition of cold ethanol and precipitation of the DNA (or by freeze-drying and lyophilization). The resulting DNA material was resuspended in 5 μ L of an 80% formamide solution containing tracking dyes, heated at 90 °C for 4 min, and chilled in ice for 4 min prior to electrophoresis on polyacrylamide gels under denaturing conditions (8% acrylamide containing 8 M urea). After electrophoresis, gels were soaked in 10% acetic acid for 10 min, dried, and analyzed as previously described.

Ion-Spray Mass Spectrometry. For the study of DNA alkylation, a 7-bp hairpin oligonucleotide d(CTATGACTCT-GTCATAG) (duplex underlined) (50 μ M) was incubated at 20 °C alone or with 50 μ M of S23906-1 compound in 1 mM ammonium acetate (pH 7.15) in a final volume of 200 μ L. The unbound and S23906-1-complexed oligonucleotides were separated from the free S23906-1 compound by a phenol/chloroform extraction followed by an ethanol precipitation. The dried pellets were dissolved in solution containing 50% acetonitrile and 1% triethanolamine in water, and the samples were injected in a simple-quadrupole mass spectrometer API I (PerkinElmer Sciex, PerkinElmer, Shelton, CT) equipped with an ion-spray (nebulizer-assisted electrospray) source (Sciex, Toronto, Canada). The solutions were continuously infused with a medical infusion pump (Model 11, Harvard Apparatus, South Natick, MA) at a flow rate of 5 μ L/min. Poly propylene glycol (PPG) was used to calibrate the quadrupole. Ion-spray mass spectra were acquired at unit resolution by scanning from *m/z* 500 to 1500 with a step size of 0.1 Da and a dwell time of 2 ms. Ten spectra were summed and recorded at an orifice voltage of -60 V, whereas the potential of spray needle was held at -4.5 kV.

For the study of S23906-1 hydrolysis, 100 μ M of S23906-1 was incubated for 2 h at 20 °C in 200 μ L of 1 mM ammonium acetate (pH 7.15) prior to injection. Ion-spray mass spectra were acquired at unit resolution by scanning from *m/z* 350 to 550 with an orifice voltage of +80 V and potential of spray needle held at +5 kV.

Alkylation of Oligonucleotides and Fluorescence Measurements. Compounds S23906-1 and S23907 (25 μ M) were incubated with or without the double-stranded oligonucleotides (10 μ M) containing A•T, G•C, or I•C as single type of base pairs in 100 μ L of incubation buffer (1 mM sodium cacodylate (pH 7.0)) for 15 h at room temperature. Free drug molecules were separated from DNA-cross-linked molecules by a phenol/chloroform/isoamyl alcohol (25:24:1) extraction followed by the addition of 5 μ L of 5 M NaCl and precipitation of DNA using 1 mL of 100% ethanol at -20 °C. After centrifugation at 13 000 rpm for 30 min, the DNA pellet was dried and dissolved in 1 mL of incubation buffer. The fluorescence of the compound covalently linked to DNA was measured using an excitation wavelength of 354 nm and an emission range from 450 to 670 nm.

¹ Abbreviations: bp; base pair; TBE, tris-borate-EDTA.

For the kinetic measurements, compounds S23906-1, S28687, or S23907 (5 μ M) were incubated with or without the AT, GC, or IC double-stranded oligonucleotides (0.4 μ M) in 1 mL of binding buffer (1 mM sodium cacodylate (pH 7.0)), and the fluorescence of the compound was measured at different times after the addition of nucleic acid (excitation wavelength 354 nm, and emission at 510 nm).

Cell Cultures. B16 melanoma cells were grown in DMEM-glutaMAX medium (Gibco, Invitrogen, Carlsbad, CA) supplemented with 10% fetal calf serum (FCS), penicillin (100 IU/mL) and streptomycin (100 μ g/mL) in a humidified atmosphere at 37 °C under 5% CO₂. B16 cells were harvested by trypsinization and plated 24 h before treatment with the test drug.

Detection of S23906-1–DNA Adducts in B16 Melanoma Cells. A total of 1.5×10^6 B16 cells were grown for 24 h prior to the addition of increasing concentrations of S23906-1 (1–40 μ M) for 24 h. Cells were then collected by centrifugation (1300 rpm, 5 min), washed twice with 10 mL PBS buffer, and resuspended in 2 mL of PBS containing 5 mM MgCl₂ prior to the addition of 200 μ L of 10% SDS and mild agitation for 5 min. Proteinase K (80 μ L at 10 mg/mL) was added for a further 5 min of mild agitation, finally 200 μ L of 0.1 M EDTA (pH 7.5) was added, and the mixture was incubated 4 h at 37 °C. After addition of 80 μ L 5 M NaCl, the DNA was extracted using 3 mL of phenol/chloroform/isoamyl alcohol (25:24:1) and centrifugation at 4000 rpm for 10 min, followed by two extractions with 3 mL of chloroform/isoamyl alcohol (24:1). Finally, the DNA was precipitated with cold ethanol and centrifugation at 11 000 rpm for 30 min. The dry pellet was then dissolved in 200 μ L H₂O and treated for 2 h with 5 μ M of RNase A (10 mg/mL) to avoid RNA contamination. The absorption of the final solution was measured at 260 nm to estimate the quantity of collected DNA. The fluorescence of S23906-1 covalently linked to DNA was measured using a SPEX Fluorolog spectrofluorimeter with an excitation wavelength at 300 nm and an emission range from 450 to 560 nm.

Confocal Microscopy. B16 melanoma cells were incubated with 10 μ M S23906-1 for 12 h at 37 °C. The medium was then removed, and the cells were rinsed for 10 min with ice-cold PBS prior to fixation with 2% paraformaldehyde for 20 min at 4 °C. After washing, a drop of anti-fade solution containing the dye TOTO-3 (100 nM, Molecular Probes, Eugene, OR) was added. The fluorescence of the drug was recorded by confocal microscopy using a Leica DMIRBE microscope controlled by a Leica TCS-NT workstation (Leica Microsystems, Bensheim, Germany) with a 63 \times 1.32 NA oil objective, equipped with a 75 mW argon–krypton laser line. The emission signal was observed through a dichroic mirror (DD488/568) followed by a filter set (RSP 580, BF 530/30, BP 600/30). The optical sections were obtained in the Z axis and stored on the computer with a scanning mode.

RESULTS

S23906-1 Does Not Intercalate DNA and Does Not Inhibit Topoisomerases. The benzoacronycine derivative S23906-1 presents a planar chromophore susceptible to insert between two consecutive base pairs of DNA to form intercalation complexes. However, DNA relaxation experiments per-

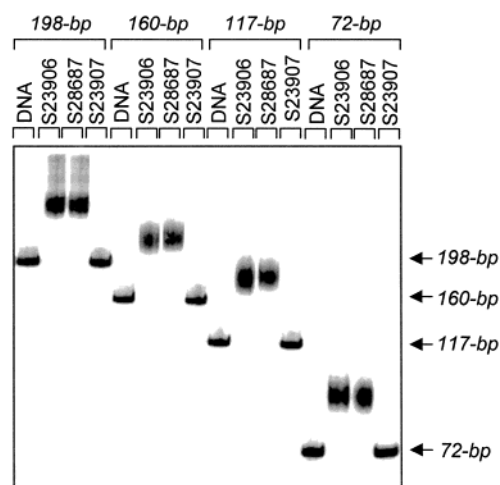


FIGURE 2: Covalent binding of S23906-1 and S28687 to DNA. The indicated drug (20 μ M each) was incubated with a radiolabeled DNA fragment of 72, 117, 160, or 198 bp for 15 h at room temperature prior to electrophoresis on nondenaturing 6% polyacrylamide gels. Control tracks labeled “DNA” contained no drug.

formed with supercoiled DNA showed that neither the diacetate derivative S23906-1 nor the monoacetate derivative S28687 or the diol derivative S23907 affect the topoisomerase I-mediated relaxation of plasmid DNA. Absorption measurements also indicated that the three compounds only weakly stabilize double-stranded DNA against heat denaturation. The melting temperature of calf thymus DNA is unchanged in the presence of S23907 and only slightly increased in the presence of S23906-1 ($\Delta T_m < 3$ °C at a 1:1 drug–DNA base pairs ratio). Circular and linear dichroism measurements on S23907–DNA complexes also showed no evidence of intercalation. In addition, we observed that the three benzoacronycine derivatives tested here do not stabilize DNA–topoisomerase (I or II) covalent complexes (data not shown).

S23906-1 Binds Covalently to DNA. Gel shift experiments were performed with four different DNA fragments to provide an assessment of the selectivity of the three benzoacronycine derivatives with respect to a wide variety of potential binding sites. The 3'-end-radiolabeled DNA fragments of 72, 117, 160, and 198 base pairs were incubated overnight with the test compounds at 20 μ M in a standard cacodylate binding buffer at pH 7.0 prior to loading the samples on a polyacrylamide gel under nondenaturing conditions. As shown in Figure 2, the diol S23907 did not perturb the migration of the DNA fragments in the gel, whereas both the mono- and diacetate derivatives strongly reduced the electrophoretic mobility of the different DNA. No effect was observed with the diol S23907 or with acronycine, even at a concentration as high as 100 μ M (data not shown). This first set of experiments provides direct evidence that S28687 and S23906-1, but not S23907, interact strongly with DNA, and this observation prompted us to investigate the effects of the drug concentration (Figure 3), the kinetic of the reaction (Figure 4), and the influence of the temperature (Figure 5).

When a ³²P-radiolabeled DNA fragment of 117 bp was incubated with increasing concentrations of S23906-1 for 1 h prior to electrophoresis, no shift was observed. However, when the drug was incubated with DNA for a longer period of 15 h, then a prominent shift was clearly detected,

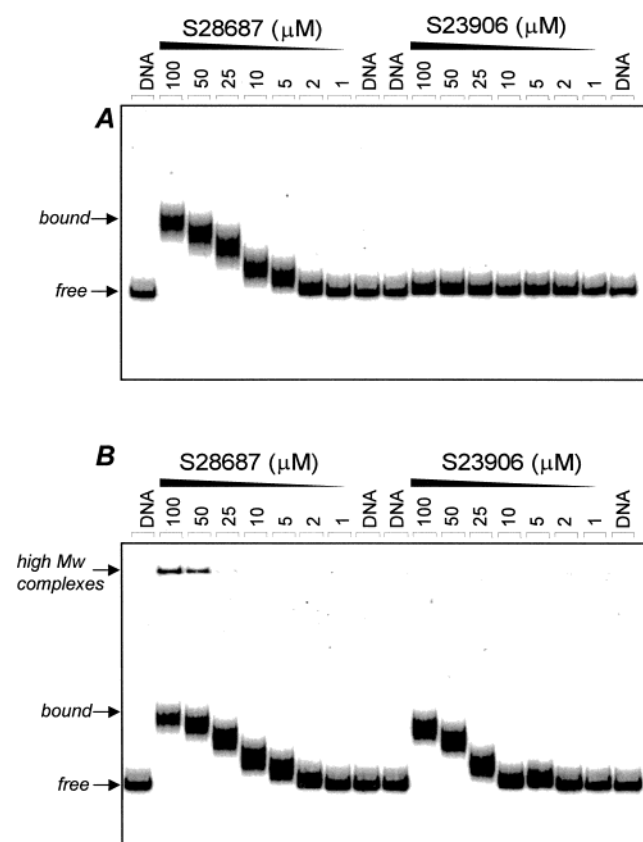


FIGURE 3: Concentration dependence for the alkylation of DNA by S23906-1 and S28687. The drug was reacted with a 117-bp radiolabeled DNA from plasmid pBS for (A) 1 h or (B) 15 h at room temperature prior to electrophoresis on nondenaturing 6% polyacrylamide gels. The concentration (μM) of the drug is shown at the top of the appropriate gel lanes. Control tracks labeled "DNA" contained no drug.

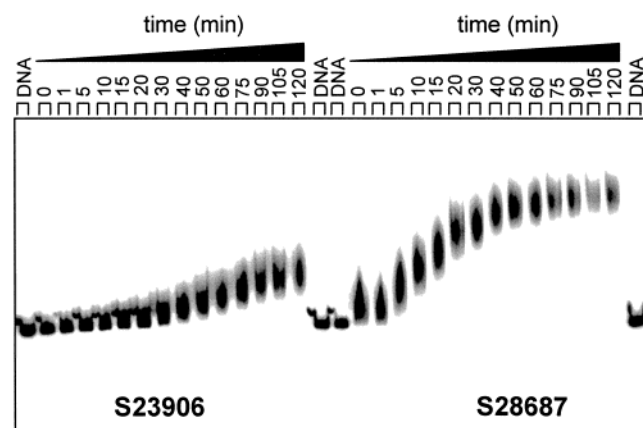


FIGURE 4: Time dependence for the alkylation of DNA by S23906-1 and S28687. The drug ($50 \mu\text{M}$) was reacted with the 117-bp DNA for up to 2 h at room temperature prior to electrophoresis on a nondenaturing 6% polyacrylamide gel. Control tracks labeled "DNA" contained no drug.

suggesting a tight attachment of the drug to DNA (Figure 3). With the monoacetate derivative S28687, the shift was already very important after 1 h incubation, and after 15 h, a small amount of DNA was detected at the top of the gel, indicating the formation of high molecular weight complexes. These large complexes, also detected under denaturing conditions (see Figure 7), may reflect to the formation of cross-linked DNA molecules, but experiments performed

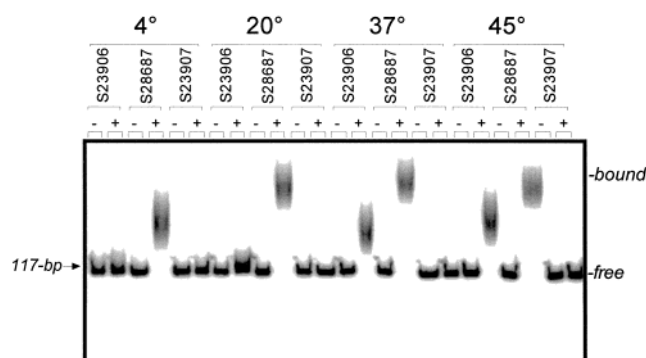


FIGURE 5: Temperature dependence for the alkylation of DNA by S23906-1 and S28687. The drug ($50 \mu\text{M}$) was reacted with the 117-bp DNA for 1 h at the indicated temperature ($^{\circ}\text{C}$) prior to electrophoresis on a nondenaturing 6% polyacrylamide gel.

with plasmid DNA suggest that the drug essentially forms monoadducts. Both S28687 and S23906-1 reduce the electrophoretic mobility of supercoiled DNA, but the drug–plasmid DNA complexes can still be fully relaxed in the presence of topoisomerase I. The enzyme activity is characterized by conversion of pKS plasmid DNA from the supercoiled conformation (Sc, form I) to the relaxed conformations (topoisomers) (Figure S1, Supporting Information). Further studies are in progress to try to identify the nature of these high molecular weight complexes.

The data in Figure 3 suggest that the monoacetate compound S28687 reacts with DNA more rapidly than the diacetate derivative S23906-1. This is fully confirmed by the kinetic data presented in Figure 4. The shift observed after 10 min with S28687 is roughly equivalent to that observed with S23906-1 after 90 min. There is no doubt that the monoacetate compound is significantly more reactive than the diacetate analogue. The temperature is also an important parameter to consider. At 4°C , S28687, but not S23906-1, retarded the mobility of the DNA substrate. Under the experimental conditions used in Figure 5, the shift is observed with S23906-1 when the temperature reaches 37°C and becomes slightly more important at 45°C . The effect of the pH was also investigated, but we found no difference between pH 6.4 and 10.8 (data not shown). Altogether, the results shown in Figures 3–5 attest that the monoacetate derivative S28687 is significantly more reactive toward DNA than the diacetate S23906-1.

S23906-1–DNA complexes could not be dissociated by addition of excess nonradioactive DNA or in the presence of a high salt concentration. A $50 \mu\text{M}$ solution of S23906-1 was mixed with the 3'-end-labeled DNA, and the samples were incubated for 15 h at room temperature prior to the addition of increasing concentrations of unlabeled DNA (Figure 6A) or NaCl (Figure 6B) or KCl (not shown). In all of these cases, no dissociation of the S23906-1–DNA complexes was observed, consistent with the formation of covalent drug–DNA adducts. Dissociation could only be detected when the radioactive DNA was mixed first with an excess of cold DNA or with large amounts of NaCl and incubated for 15 h prior to adding $50 \mu\text{M}$ S23906-1. These experiments indicate that, once formed, S23906-1–DNA complexes are very stable and cannot be dissociated. Again, this is entirely compatible with the formation of covalent drug–DNA complexes.

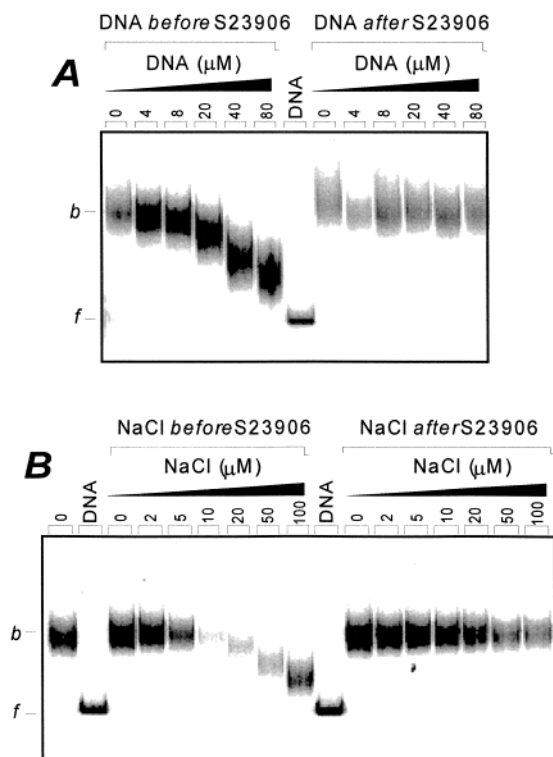


FIGURE 6: Increasing concentrations of (A) competitor DNA (nonradioactive pBS plasmid) or (B) NaCl were added to the radioactive DNA substrate before or after addition of the drug S23906-1 at 50 μM. In the first case (before), the ^{32}P -DNA substrate was incubated with the competitor DNA or the NaCl for 15 h prior to adding S23906-1, and then the solutions were kept at room temperature for another 2 h period before loading the solution on an electrophoresis gel. In the second case (after), the radioactive DNA substrate and the drug solutions were incubated for 15 h at room temperature followed by 2 h with the cold DNA or NaCl prior to electrophoresis. Symbols *f* and *b* refer to the free and drug-bound DNA species, respectively.

The covalent binding of S23906-1 to DNA was also followed by mass spectrometry using a short (7-bp) hairpin oligonucleotide. The mass spectrum of the free duplex shows well-resolved peaks at $m/z = 680.1$, 777.3, 907.1, 1088.6, and 1361.1 (Figure 7A), corresponding to the expected mass of 5448 for this sequence. Incubation of this duplex with S23906-1 for 15 h results in the formation of a mixture of 1:1, 2:1, and a small amount of 3:1 drug–DNA covalent complexes as a monoacetate form which can be easily identified by their respective mass (Figure 7B). The respective amount of each complex depends on the drug/oligonucleotide ratio. Under the experimental conditions used here, the oligonucleotide molecules with three drug molecules covalently bound to DNA are more difficult to detect and represent less than 10% of the total complexes whereas the 2:1 complexes represent about 20% of the total material detected by ESI-MS. Interestingly, we were able to detect a maximum of 3 molecules bound per oligonucleotide which contains three paired guanines residues. In contrast, as indicated in Figure 7, only 1:1 drug–DNA complexes were observed when using a related oligonucleotide bearing only one G on the 3' end. The replacement of the two G·C bp with two A·T bp limits the formation of covalent complexes. This is an indirect indication suggesting that the drug reacts with guanines, as demonstrated in the following section.

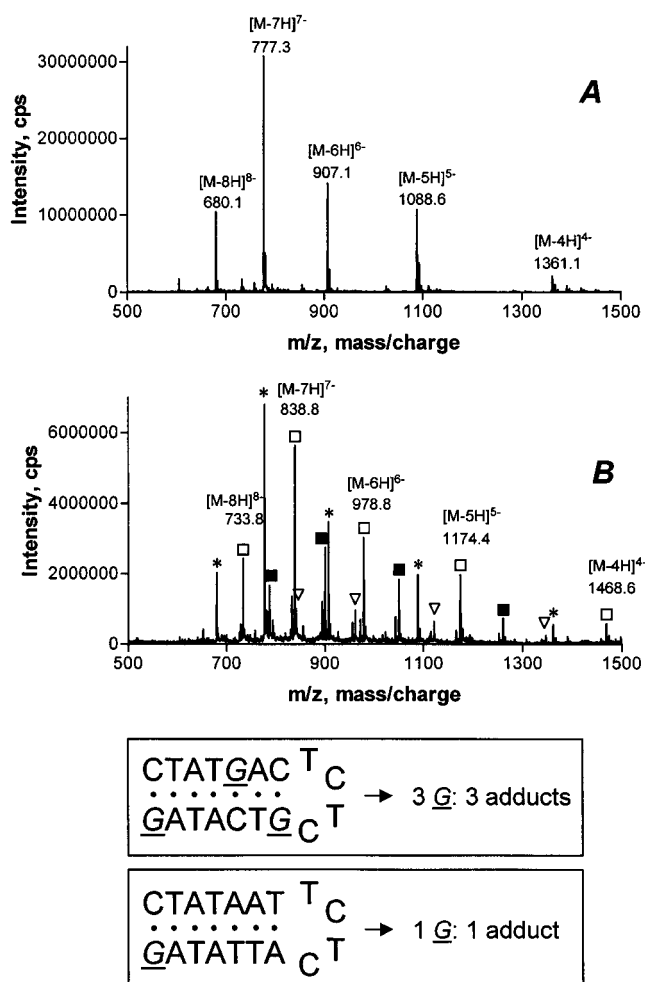


FIGURE 7: Electrospray ionization mass spectra of (A) the drug-free hairpin oligonucleotide d(CTATGACTCTCGTCATAG) (duplex underlined) and (B) the oligonucleotide–S23906-1 adducts (negative ion mode). Deconvolution of spectrum B shows the presence of four species: (*) the uncomplexed oligonucleotide and (□) 1:1, (■) 2:1, and (▽) 3:1 drug–DNA covalent complexes. The oligonucleotide ($M = 5448$) binds covalently one ($M = 5878$), two ($M = 6308$), or three ($M = 6738$) drug molecules.

Alkylation of Guanine Residues by S23906-1. The DNA sequence preference of S23906-1 was evaluated by a combination of DNase I footprinting experiments and by comparing the patterns of alkylation of single-end-labeled DNA on denaturing polyacrylamide gels. As described previously, the drug was reacted with the radioactive DNA fragment for 15 h, and the samples were ethanol-precipitated prior to electrophoresis on sequencing gels. The diol S23907 showed no effect on the electrophoretic mobility of DNA, whereas the diacetate S23906-1 strongly altered this even under denaturing conditions (Figure 8). Only a few cleavage products (migrating faster than free DNA) were detected. Using the phosphorimager, the bands corresponding to the cleavage products were intensified, and the positions of the cleavage products, by reference to the G tract, were identified on the overexposed gel. The groups of DNA bands detected in the presence of S23906-1 are not well-resolved, but nevertheless it can be easily seen that their electrophoretic mobility coincides perfectly with those of the G bands. For example, the three sets of bands in the middle of the gel correspond to the position of three GGG sequences, taking into account a slight 5' shift due to the drug-induced decrease

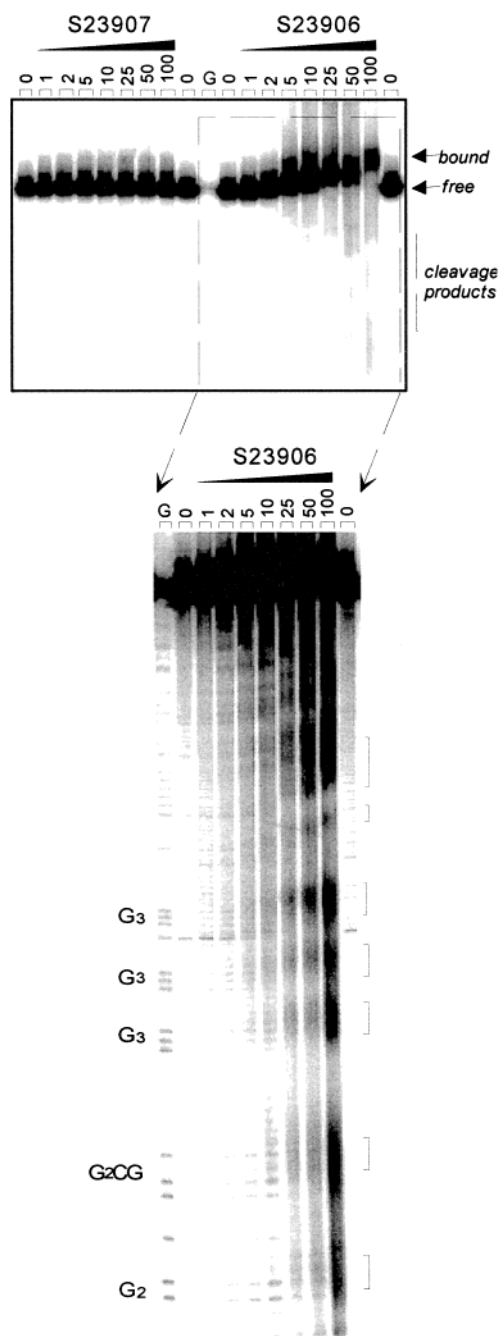


FIGURE 8: DNA alkylation patterns with S23906-1 and S23907. The 174-bp radiolabeled DNA substrate was incubated for 15 h with increasing concentrations of the test drug, from 1 to 100 μ M as indicated. The DNA was precipitated with ethanol, washed, and resuspended in loading buffer prior to electrophoresis on a 8% denaturing polyacrylamide gel. The portion of the gel boxed was overexposed on the phosphorimager to identify the principal cleavage products which all coincide with the position of GC-rich sequences, identified with respect to the positions of the Maxam–Gilbert G tracks (lanes marked G).

in mobility (Figure 8). The results suggest that S23906-1 reacts primarily with guanines. It is important to note that the treatment of the alkylated DNA samples with hot piperidine had no effect on the electrophoretic mobility of the bands and the gel resolution. The alkylation sites cannot be converted to strand breaks as is usually the case with conventional alkylators such as nitrogen mustards. The fact that S23906-1–DNA adducts are not alkali labile indicates that the reactive site is not the N7 of guanine in the major

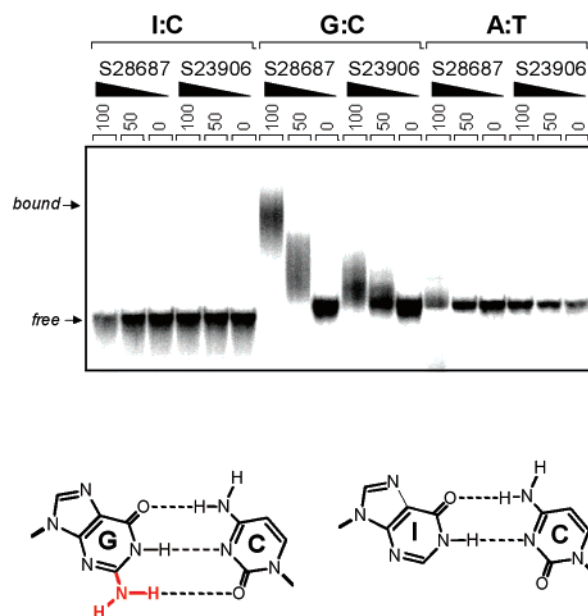


FIGURE 9: Formation of adducts with GC bp. S28687 and S23906-1 (50 or 100 μ M) were incubated with the 30-mer end-labeled oligonucleotides containing A·T, G·C, or I·C base pairs only. After 15 h incubation at room temperature, the DNA samples were precipitated with ethanol and then separated on a nondenaturing 10% polyacrylamide gel. Control track labeled “0” contained no drug. The structures of hydrogen-bonded G·C and I·C base pairs are indicated. Broken lines represent hydrogen bonds. The 2-amino group which distinguishes a G·C pair from an I·C pair is printed in red.

groove. This conclusion is also supported by dimethyl sulfate (DMS) interference assay showing that N7 guanines in DNA alkylated by S23906-1 remain fully accessible to DMS. In other words, S23906-1 does not interfere with DMS-induced methylation of guanines in the major groove (data not shown).

DNase I footprinting experiments also indicated that the drug binds preferentially to GC-rich sequences (Figure S2). In the absence of DNase I, only a few cleavage products can be detected, and they correspond to GC tracts. In the presence of DNase I, the cleavage essentially occurs at AT-rich sequences, whereas the cutting at GC tracts is reduced. The footprints are not well resolved due to S23906-1-induced alkylation of DNA and decreased electrophoretic mobility of the DNA. However, the two approaches, DNA alkylation and DNase I footprinting, both indicate that S23906-1 reacts primarily with guanines.

The 2-Amino Group of Guanine Is Required for Covalent Complex Formation. We then used 30-mer end-labeled oligonucleotides to further characterize S23906-1 binding to DNA. To simplify the system, we prepared duplexes containing only one type of base pairs: A·T or G·C, or I·C. Inosine (I) is a base analogue of guanine lacking the 2-amino group, which is the only hydrogen bond donor group exposed in the minor groove of double-helical DNA. Inosine pairs with cytosine, engaging in two hydrogen bonds of the Watson–Crick type (Figure 9). S28687 and S23906-1 were incubated with each duplex for 15 h, the samples were extracted with phenol to remove unbound drug molecules, and the DNA was precipitated with ethanol prior to electrophoresis on 12% polyacrylamide gel under nondenaturing conditions. As shown in Figure 9, drug-induced gel retarda-

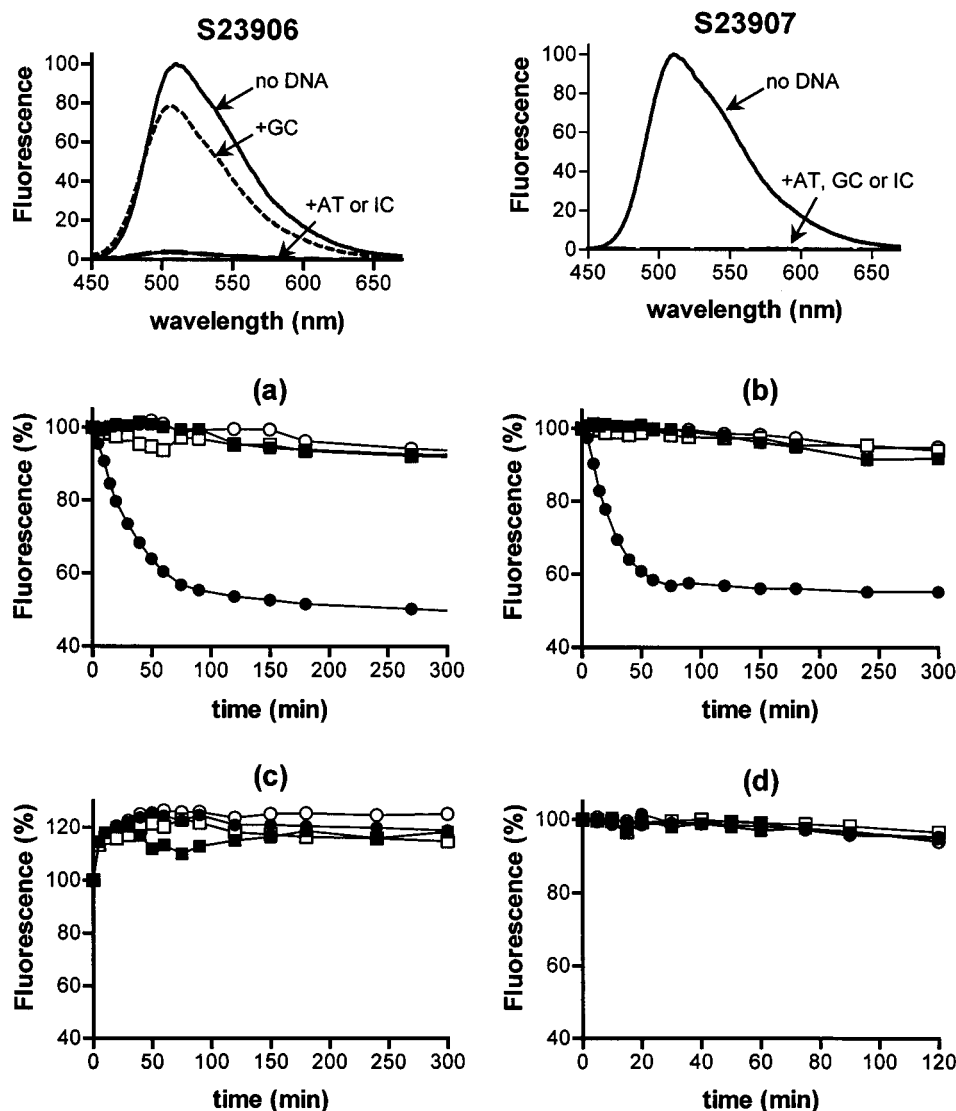


FIGURE 10: Fluorescence emission spectra of S23906-1 (2.5 μ M, solid line) in the absence of DNA and in the presence of the AT, GC, or IC oligonucleotides. Except for drug alone, all spectra were recorded after phenol extraction of the noncovalently bound molecules and further ethanol precipitation of the nucleic acids. The other panels show a kinetic study of the reactivity of S23906-1, S28687, and S23907 with the 30-mer oligonucleotide duplexes containing A•T, G•C, or I•C base pairs only. In each case, the drug (5 μ M) was incubated (○) without or with the (■) AT, (●) GC, or (□) IC oligonucleotides (0.4 μ M each) in 1 mM sodium cacodylate, pH 7.0. The fluorescence (excitation 354 nm, emission 510 nm) was recorded over a period of 5 h and expressed as the percentage of the measured fluorescence over the initial fluorescence of the compound measured before the addition of the nucleic acid.

tion was observed with the GC oligonucleotide, whereas no detectable effect was observed with either the AT or with the IC oligonucleotides. The differential reactivity of S28687 and S23906-1 between the GC and IC duplexes strongly suggests that the drug reacts with the amino group at position 2 of guanine from the DNA minor groove.

We investigated further the G-specific reactivity by fluorescence spectroscopy. The intrinsic fluorescence of the benzoacronycine chromophore is particularly convenient to evaluate the interaction of the drug with the different DNA duplexes. S23906-1 fluoresces in the 500–550 nm region upon excitation at 354 nm, and the addition of calf thymus DNA induces a marked quenching of the fluorescence, which is useful to monitor the drug–DNA interaction process (Figure S3).

S23906-1 was incubated overnight with each duplex, and then the unbound molecules were removed by phenol/chloroform extraction. The fluorescence spectra were com-

pared with that of the drug at the same concentration (2.5 μ M) in the absence of DNA (Figure 10). In the presence of the GC oligonucleotide, the fluorescence emission at 510 nm is nearly the same as the nonextracted control, whereas practically no fluorescence was detected with both the AT and IC oligonucleotides. No fluorescence was detected in the DNA samples incubated with the diol compound S23907 (data not shown). Thus, the acetate groups of S23906-1 are essential to the reaction with guanines.

The kinetics of the reactions between the drugs and the oligonucleotides were followed by fluorescence, and the results (Figure 10) confirmed that the reaction can only occur between S23906-1 or S28687 and the GC duplex. In this case, the fluorescence was directly recorded without phenol extraction. The fluorescence intensity does not vary upon addition of these mono- or diacetate compounds to the AT and IC oligonucleotides, whereas a large decrease of fluorescence is observed with the GC oligonucleotide. The

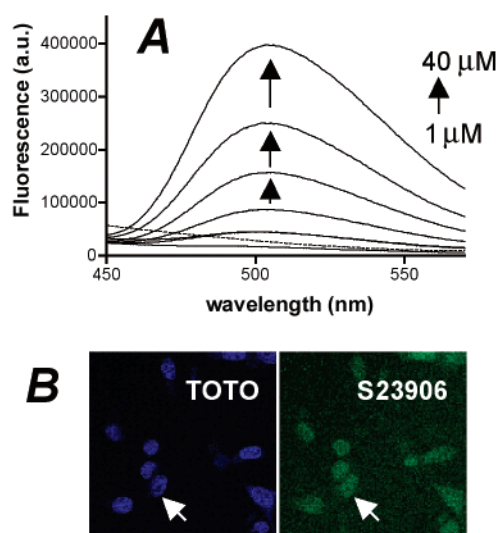


FIGURE 11: Formation of drug–DNA covalent complexes in cells. (A) Fluorescence emission spectra of DNA extracted from B16 melanoma cells treated with graded concentrations of S23906-1 (1, 2.5, 5, 10, 20, 40 μ M, bottom to top curves at 500 nm). The dashed line corresponds to the untreated control. The excitation wavelength was 300 nm. (B) Laser-scanning confocal microscopy of S23906-1-treated B16 melanoma cells showing the green fluorescence of the nucleus. Cells were incubated with 10 μ M S23906-1 for 12 h at 37 $^{\circ}$ C prior to washing with buffer, counterstaining with the dye TOTO-3 (100 nM), and cytocentrifugation.

reaction is relatively slow. It takes about 2 h to reach the equilibrium where the fluorescence is maintained at a constant level. With the diol S23907, similar effects were observed with all three duplexes containing either A•T, G•C, or I•C pairs. A rapid 20% increase of the fluorescence emission was observed and remains constant (even after 24 h). Additional experiments performed with the most reactive compound, the monoacetate S28687, in the presence of either dGTP, dCTP, or the dinucleoside CG-5',3'-P showed no quenching of the fluorescence (data not shown). The covalent binding was only observed with the 30-mer duplex GC oligonucleotide. These different experiments confirm that S28687 and S23906-1, but not S23907, forms covalent complexes with DNA, and we concluded that the alkylation of DNA by S23906-1 requires the presence of guanine 2-amino group.

Formation of S23906-1–DNA Covalent Complexes in Cells. The previous experiments establish that S23906-1 can bind covalently to purified DNA. To verify the formation of DNA adducts in whole cells, B16 melanoma cells were treated with 1 to 40 μ M S23906-1 for 15 h. The genomic DNA was subsequently isolated by phenol extraction and precipitated prior to investigation of drug–DNA adducts, using the same fluorescence method as used previously for the experiments with purified DNA and polynucleotides. As shown in Figure 11A, the fluorescence spectra of DNA solution obtained from the B16 cells treated with S23906-1 reveal unambiguously the presence of drug molecules attached to the genomic DNA. Similar experiments performed with the diol S23907 and acronycine showed no fluorescence associated with the DNA. Further experiments showed that the fluorescence intensity of the genomic DNA solutions obtained from S23906-1-treated cells was concentration- and time-dependent. The DNA-associated fluorescence of S23906-1 can be detected as soon as 30 min after

addition of the drug (40 μ M) to cells, and similar results were obtained with different human tumor cell lines such as HT-29 colon carcinoma (data not shown).

The presence of S23906-1 molecules in the nuclei of whole cells was confirmed by confocal microscopy. Nuclei of B16 cells treated with S23906-1 appeared in green under the fluorescence microscope (Figure 11B). When the cells were counter stained with the blue dye TOTO-3, as a probe for cellular DNA, we found identical distribution profiles for the two fluorochromes. The perfect superimposition of the two images obtained with TOTO-3 and S23906-1 establishes that the benzoacronycine derivative effectively accumulates into the nucleus of the B16 cells. The two sets of experiments shown in Figure 11 show that S23906-1 concentrates in the nucleus to form stable adducts with DNA.

DISCUSSION

The aim of this study was to identify the molecular target for the synthetic compound S23906-1, a benzoacronycine derivative which has demonstrated potent, unusual, and selective *in vivo* activity in experimental models of human solid tumors (8). Because of the presence of planar, unsaturated rings in the structure of S23906-1, we first envisaged that it could intercalate DNA and inhibit topoisomerases. Surprisingly, complementary biochemical and biophysical measurements showed no sign of intercalation of S23906-1 into DNA prior to covalent binding. In addition, both DNA relaxation and cleavage experiments using plasmid DNA and restriction fragments, respectively, indicated that the drug does not stabilize DNA–topoisomerase I or II covalent complexes. The lack of intercalation and inhibition of topoisomerases distinguishes S23906-1 from conventional DNA-binding antitumor drugs, such as acridines or anthracyclines. However, S23906-1 binds to DNA. Having observed, in preliminary experiments, that S23906-1 retarded the electrophoretic migration of DNA fragments, we decided to investigate further for formation of S23906-1–DNA complexes.

All of the data reported here, be it with purified DNA or with DNA extracted from tumor cells exposed to S23906-1, indicate that the drug forms covalent complexes with DNA. This property is unexpected, considering the structure of this acronycine derivative. The demonstration of the point of covalent attachment between S23906-1 and DNA is an essential first step in investigating the structural and biological consequences of DNA modification. A series of experiments was undertaken to first establish that the drug binds covalently to DNA, including in a cellular context, then to show that guanines are selectively alkylated, and finally to identify the guanine 2-amino group as the potential reactive site. These experiments provide circumstantial evidence for the requirement of the 2-amino group in the covalent reaction.

A similar approach (in particular using inosine-containing DNA substrates) has been used previously to characterize the N2-G specificity of mitomycin C (14), anthramycin (15), and ecteinascidin 743 (hereafter named Et743) (16). The inability of S23906-1 to form a covalent adduct with the IC oligonucleotide contrasts with the strong binding to the corresponding GC duplex. The possibility of covalent binding through N7 of guanine can be eliminated by the unaltered

reactivity toward dimethyl sulfate of S23906-1-alkylated DNA. Moreover, treatment of the DNA–S23906-1 complexes with hot piperidine showed no DNA breaks. The stability of the *N*-glycosidic linkage of the covalent modified guanine to alkaline hydrolysis is consistent with alkylation at the N2 position of guanine, which does not disturb the purine aromaticity (17). Collectively, the results demonstrate that S23906-1, as well as its monoacetate analogue S28687, binds covalently to guanines via the exocyclic 2-amino group which resides in the minor groove of B-form DNA.

The diol derivative S23907 lacking the two acetate groups is devoid of antitumor properties, both in vitro and in vivo. This compound failed to yield covalent DNA adducts, providing the first evidence that (i) the C1–C2 functionality of S23906-1 is the DNA reactive moiety and (ii) the unique pharmacological profile of this compound could be due to its DNA alkylating properties. Acronycine itself, as well as benzoacronycine, contains a C1=C2 double bond and does not alkylate DNA, at least in vitro. It is possible that, in vivo, acronycine is activated into a DNA-reactive intermediate. Small quantities of the unstable acronycine C1–C2 epoxide have been isolated from several New Caledonian *Sarcome-licope* species, leading thus to the hypothesis of bioactivation of acronycine by transformation of the 1,2-double bond into the corresponding oxirane in vivo (18).

Mechanistically, the mode of DNA alkylation of S23906-1 is shared by a small group of DNA reactive molecules. In the case of Et743 (19, 20) and related carbinolamine antibiotics, as well as the pyrrolo[1,4]benzodiazepine antibiotics (21), the formation of N2-guanine adducts involve an intermediate iminium ion generated from the carbinolamine function. N2-guanine adducts have also been identified with the antitumor agent mitomycin C through opening of its reactive aziridine moiety (22), with the benzopyrenediol epoxide which is a highly tumorigenic metabolite of the environmental toxin benzo[*a*]pyrene (23), and with the nonsteroidal anti-estrogen drug tamoxifen (24). The structure of S23906-1 is very distinct from that of these drugs, and the reactive intermediate must be quite different. Among these molecules, only mitomycin C and Et743 have clearly shown antitumor activity in the clinic.

It is interesting to compare the structure of S23906-1 with that of mitomycin C and two simplified analogues DHRA and BAMP (Figure S4) related to plant-derived pyrrolizidine alkaloids and which can all react with the guanine 2-amino group. The aziridomitosene of mitomycin C bridges the exocyclic amino groups of two guanine residues by sequential formation and reaction with DNA electrophilic sites at carbons 1 and 10 of the mitosene (25, 26). Dehydroretronecine diacetate (DHRA) bears reactive functionality at carbons 7 and 9 capable of sequential reactivity analogous to that at carbons 1 and 10 of an aziridomitosene (27). A N2-deoxyguanosine-C7-dehydropyrrolizidine conjugate has been isolated (28), providing thus strong support for a similar mechanism of DNA cross-linking reactions of mitomycins and pyrrolizidine alkaloids. A simple mitosene analogue such as 2,3-bis(acetoxymethyl)-1-methylpyrrole (BAMP), in which carbons 2' and 3' bear analogy to sites 1 and 10 of mitomycin, also forms N2-guanine adducts (27). The striking similarity between the acetate functionality at position C1 for S23906-1, C7 for DHRA and C2' for BAMP is entirely consistent with a similar mechanism of action. It is important

to mention that, unlike mitomycin C but like S23906-1, DHRA and BAMP do not require reductive activation for cross-linking.

These different considerations lead us to propose a potential reaction scheme for the formation of S23906-1-C1–guanine-N2 adducts as shown in Figure 1. The proposed mechanism involves nucleophilic attack by the 2-NH₂-G on the C1 carbon bearing the acetate adjacent to the *N*-methyl group. This acetate group is ideally positioned with respect to the acridinone moiety to act as a leaving group for the subsequent formation of a reactive species susceptible to nucleophilic attack by the 2-NH₂-G. The 1-deacetyl DNA-reactive form of S23906-1 may result from the formation of a *N*-methyl iminium intermediate comparable to the iminium intermediate postulated for drugs such as BAMP (27), Et743 (16, 20), as well as the pyrrolo[1,4]benzodiazepine anthracycline (29) or tomaymycin (30). Interestingly, this potential mechanism accounts satisfactorily for the structure–activity relationships available in the benzoacronycine series in that the derivatives bearing a NH acridinone are generally less cytotoxic than their *N*-methyl acridinone counterparts (7). The proposed formation of S23906-1-C1–N2-guanine adducts (Figure 1) is also fully consistent with the mass spectrometry data (Figure 7). The fact that the guanine amino group reacts with the carbon bearing the leaving acetate group at position 1 is supported by molecular modeling and structure–activity relationship studies. For example, compounds bearing a nonleaving group at position C1 (e.g., a methoxy or a keto group) and an acetate at C2 do not form covalent adducts with DNA. A detailed mechanistic study demonstrating that the attack occurs at C1 will be reported soon.

Although all of the data presented here clearly show the alkylation of DNA by S23906-1, the question remains whether the potent antitumor activity of this compound is the consequence of the formation of a covalent adduct with the guanine-N2 position. The fact that DNA-linked S23906-1 can be detected as soon as 30 min after incubating tumor cells with the compound is perfectly consistent with the high cytotoxicity observed after short duration of exposure (9). The lack of DNA alkylation by the diol derivative, which is devoid of cytotoxicity and antitumor activities, strongly suggest a close link between alkylation and antitumor activity in this series.

In conclusion, we have identified the synthetic drug S23906-1 as a structurally unique DNA alkylating antitumor agent. The mechanism of action of this potent, broad spectrum anticancer drug is reminiscent to that of the antibiotics mitomycin C and ecteinascidin 743, which are also potent anticancer agents forming covalent DNA minor groove adducts with guanines, but both its mode of interaction and pharmacological profile are different. The promising antitumor activity of S23906-1 in vivo coupled with its ability to produce covalent DNA minor groove adducts with both purified DNA and genomic DNA in cells open a new field for future drug design.

ACKNOWLEDGMENT

The authors thank the Service Commun d'Imagerie Cellulaire de l'IMPRT for access to the confocal microscope. We also thank Dr. E. Canet and Dr. G. Atassi for supporting

this collaboration, the team of chemists (Pr. M. Koch, Pr. F. Tillequin, Dr. S. Michel, and Dr. B. Pfeiffer) for the synthesis of acronycine derivatives, and helpful discussion regarding the potential mechanism of alkylation.

SUPPORTING INFORMATION AVAILABLE

Four Figures showing the activity of S23906-1 and S28687 with supercoiled plasmid DNA, DNase I footprinting with S23906-1, fluorescence spectral titrations of S23906-1 with calf thymus DNA, and the structures of mitomycin C, DHRA, BAMP. This material is available free of charge via the Internet at <http://pubs.acs.org>.

REFERENCES

1. Warpehoski, M. A., and Hurley, L. H. (1988) *Chem. Res. Toxicol.* **1**, 315–333.
2. Denny, W. A. (2001) *Curr. Med. Chem.* **8**, 533–544.
3. Hughes, G. K., Lahey, F. N., Price, J. R., and Webb, L. J. (1948) *Nature* **162**, 223–224.
4. Svoboda, G., Poore, G. A., Simpson, P. J., and Boder, G. B. (1966) *J. Pharm. Sci.* **55**, 759–768.
5. Dorr, R. T., Liddil, J. D., Von Hoff, D. D., Soble, M., and Osborne, C. K. (1989) *Cancer Res.* **49**, 340–344.
6. Elomri, A., Mitaku, S., Michel, S., Skaltsounis, A.-L., Tillequin, F., Koch, M., Pirr , A., Guilbaud, N., L once, S., Kraus-Berthier, L., Rolland, Y., and Atassi, G. (1996) *J. Med. Chem.* **39**, 4762–4766.
7. Costes, N., Le Deit, H., Michel, S., Tillequin, F., Koch, M., Pfeiffer, B., Renard, P., L once, S., Guilbaud, N., Kraus-Berthier, L., Pierr , A., and Atassi, G. (2000) *J. Med. Chem.* **43**, 2395–2402.
8. Guilbaud, N., Kraus-Berthier, L., Meyer-Losic, F., Malivet, V., Chacun, C., Jan, M., Tillequin, F., Koch, M., Pfeiffer, B., Atassi, G., Hickman, J. A., and Pierr , A. (2001) *Clin. Cancer Res.* **7**, 2573–2580.
9. L once, S., Perez, V., Lambel, S., Peyroulan, D., Tillequin, F., Michel, S., Koch, M., Pfeiffer, B., Atassi, G., Hickman, J. A., and Pierr , A. (2001) *Mol. Pharmacol.* **60**, 1383–1391.
10. Gout, P. W., Dunn, B. P., and Beer, C. T. (1971) *J. Cell Physiol.* **78**, 127–138.
11. Dunn, B. P., Gout, P. W., and Beer, C. T. (1973) *Cancer Res.* **33**, 2310–2319.
12. Reddy, S. B., Linden, W. A., Zywiets, F., Baisch, H., and Struck, U. (1977) *Arzneim.-Forsch.* **27**, 1549–1553.
13. Shieh, H.-L., Pezzuto, J. M., and Cordell, G. A. (1992) *Chem.-Biol. Interact.* **81**, 35–55.
14. Tomasz, M., Das, A., Tang, K. S., Ford, M. G. J., Minnock, A., Musser, S. M., and Waring, M. J. (1998) *J. Am. Chem. Soc.* **120**, 11581–11593.
15. Thurston, D. E. (1999) in *Molecular Aspects of Anticancer Drug–DNA Interactions* (Neidle, S., and Waring, M. J., Eds.) Vol. 1, pp 54–87, Macmillan, London, U.K.
16. Pommier, Y., Kohlhaagen, G., Bailly, C., Waring, M. J., Mazumder, A., and Kohn, K. W. (1996) *Biochemistry* **35**, 13303–13309.
17. Hurley, L. H., Lee, C. S., and Cheatham, S. (1986) in *Molecular Mechanism of Carcinogenic and Antitumor Activity* (Chagas, C., and Pullman, B., Eds.), pp 385–402, Adenine Press, NY.
18. Brum-Bousquet, M., Mitaku, S., Skaltsounis, A. L., Tillequin, F., and Koch, M. (1988) *Planta Med.* **54**, 470–471.
19. Moore, B. M., Seaman, F. C., Wheelhouse, R. T., and Hurley, L. H. (1998) *J. Am. Chem. Soc.* **120**, 2490–2491.
20. Seaman, F. C., and Hurley, L. H. (1998) *J. Am. Chem. Soc.* **120**, 13028–13041.
21. Boyd, F. L., Cheatham, S. F., Remers, W., Hill, G. C., and Hurley, L. H. (1990) *J. Am. Chem. Soc.* **112**, 3279–3289.
22. Gargiulo, D., Musser, S. S., Yang, L., Fukuyama, T., and Tomasz, M. (1995) *J. Am. Chem. Soc.* **117**, 9388–9398.
23. Patel, D. J. (1992) *Current Opin. Struct. Biol.* **2**, 345–353.
24. Fan, P. W., and Bolton, J. L. (2001) *Drug Metab. Dispos.* **29**, 891–896.
25. Sastry, M., Fiala, R., Lipman, R., Tomasz, M., and Patel, D. J. (1995) *J. Mol. Biol.* **247**, 338–359.
26. Tomasz, M., and Palom, Y. (1997) *Pharmacol. Ther.* **76**, 73–87.
27. Weidner, M. F., Sigurdsson, S. Th., and Hopkins, P. B. (1990) *Biochemistry* **29**, 9225–9233.
28. Robertson, K. A. (1982) *Cancer Res.* **42**, 8–14.
29. Kizu, R., Draves, P. H., and Hurley, L. H. (1993) *Biochemistry* **32**, 8712–8722.
30. Barkley, M. D., Thomas, T. J., and Maskos, K. (1991) *Biochemistry* **30**, 4421–4431.

BI020226+